

Two-dimensional microelectrophoresis in supported lipid bilayers

M. Stelzle, R. Miehlich, and E. Sackmann

Technische Universität München, W-8046 Garching, Germany

ABSTRACT We report the application of supported bilayers for two-dimensional microelectrophoresis. This method allows the lateral separation and accumulation of charged amphiphilic molecular probes in bilayers by application of an electric field parallel to the bilayer surface. Diffusion coefficient and mobility of the fluorescent probes are determined by observation of the fluorescence recovery after photobleaching (pattern bleaching). The diffusion coefficients and the mobilities of oppositely charged fluorescent probes in one bilayer can be determined independently from a single measurement. By analysis of the motion of charged and uncharged probes in one membrane one can distinguish between the motion caused by the electric field acting on the charge of individual probes and that caused by frictional forces due to electroosmosis.

INTRODUCTION

Supported lipid bilayers may be deposited onto solid substrates in such a way that they are separated from the substrate by an ultrathin water layer. These bilayers exhibit typical properties of giant vesicles and offer many advantages for studies of fundamental membrane properties. They were applied first for measurements of molecular friction and epitactic coupling between monolayers (Merkel et al., 1989) and second for the determination of two-dimensional (2-D) hydrodynamic radii of polymerized lipids (Eggl et al., 1990). Here we report the application of supported bilayers for 2-D microelectrophoresis. This technique allows the accumulation and separation of charged amphiphilic fluorescent dyes in the upper monolayer of a supported bilayer. By determination of both the diffusion coefficient and the drift velocity by the total internal reflection-fluorescence recovery after photobleaching (TIR-FRAP) method (Thompson et al., 1981; Zimmermann et al., 1990) with pattern bleaching (Smith and McConnell, 1978; Miehlich, R., and H. E. Gaub, manuscript in preparation), one can either check the validity of the Einstein relationship for the lateral movement of these molecular probes or determine their charge.

EXPERIMENTAL

Experimental set-up

Fig. 1 shows the experimental set-up used for the 2-D microelectrophoresis experiments. The bilayer is deposited onto a microslide by the horizontal dip method (Langmuir and Schaefer, 1938; Von Tscharner and McConnell, 1981) (Fig. 1 *a*). A second microslide into which a groove (10–50 μm deep, 10 mm wide, and 26 mm long) has been etched is deposited on top of the bilayer in such a way that a narrow channel is formed above the bilayer. An electric field is applied along the channel (and parallel to the bilayer plane) by application of a voltage of 0–1,000 V between the two ends of the channel via two platinum electrodes immersed in the surrounding buffer solution.

Address correspondence to E. Sackmann.

A very small channel cross-section was chosen to avoid excessive joule heating during the application of high electric field strength. Because of the low thermal conductivity k_a from the sample to the surrounding air, the dissipation of electric power even as small as 0.1 W, which is a typical figure in this type of experiments, leads to an intolerably high increase in chamber temperature T_{ch} . Therefore, it is necessary to control T_{ch} . Control was achieved by clamping the temperature T_s of the outer surface of the chamber with an electronically regulated Peltier element (Fig. 1 *b*) to a fixed value with a variation of $<0.2^\circ\text{C}$.

We avoided direct measurement of the temperature in the channel (for example, with a thermocouple consisting of evaporated metal films) because such films would considerably affect field homogeneity and might cause electrochemical reactions if they were in contact with the buffer solution.

A $\sin^2(x)$ bleaching pattern was established by focusing two intense interfering laser beams onto the sample. The fluorescence recovery is recorded by image exposure and processing as illustrated in Fig. 2. Images of the wavelike fluorescence intensity distribution $I(x, y, t_i)$ obtained after the bleaching pulse were taken by a high sensitivity nitrogen-cooled CCD camera (Wright Inc., Enfield, UK). The interval between consecutive exposures was 0.1 s. Each transient pattern $I(x, y, t_i)$ is averaged over the y -direction (Fig. 2, *left*) and the distributions $I(x, t_i)$ are plotted as a function of t (Fig. 2, *right*), resulting in a distribution $I(x, t)$.

The diffusion coefficient D and the mobility $\mu = \langle v \rangle / zeE$ ($\langle v \rangle$ = average velocity in the direction of the electric field E , ze = charge of fluorescent molecular probe) of the fluorescent molecular probe are determined by spatial Fourier analysis of the periodic intensity distribution $I(x, t)$. The directed Brownian motion of the molecular probes is determined by the diffusion equation

$$\frac{\partial c(x, t)}{\partial t} = D \frac{\partial^2 c(x, t)}{\partial x^2} - \mu zeE \frac{\partial c(x, t)}{\partial x}. \quad (1)$$

This equation is solved in the usual way by Fourier analysis:

$$c(x, t) = \sum_k c_k(t) e^{ikx}, \quad (2)$$

where the complex Fourier components are given by

$$c_k(t) = c_k^0 \exp(-ik\mu zeEt) \exp(-k^2 Dt). \quad (3)$$

Data evaluation is achieved by spatial Fourier transform of the images yielding $c(k, t)$. Then the data set $c_k(t)$ with k corresponding to the

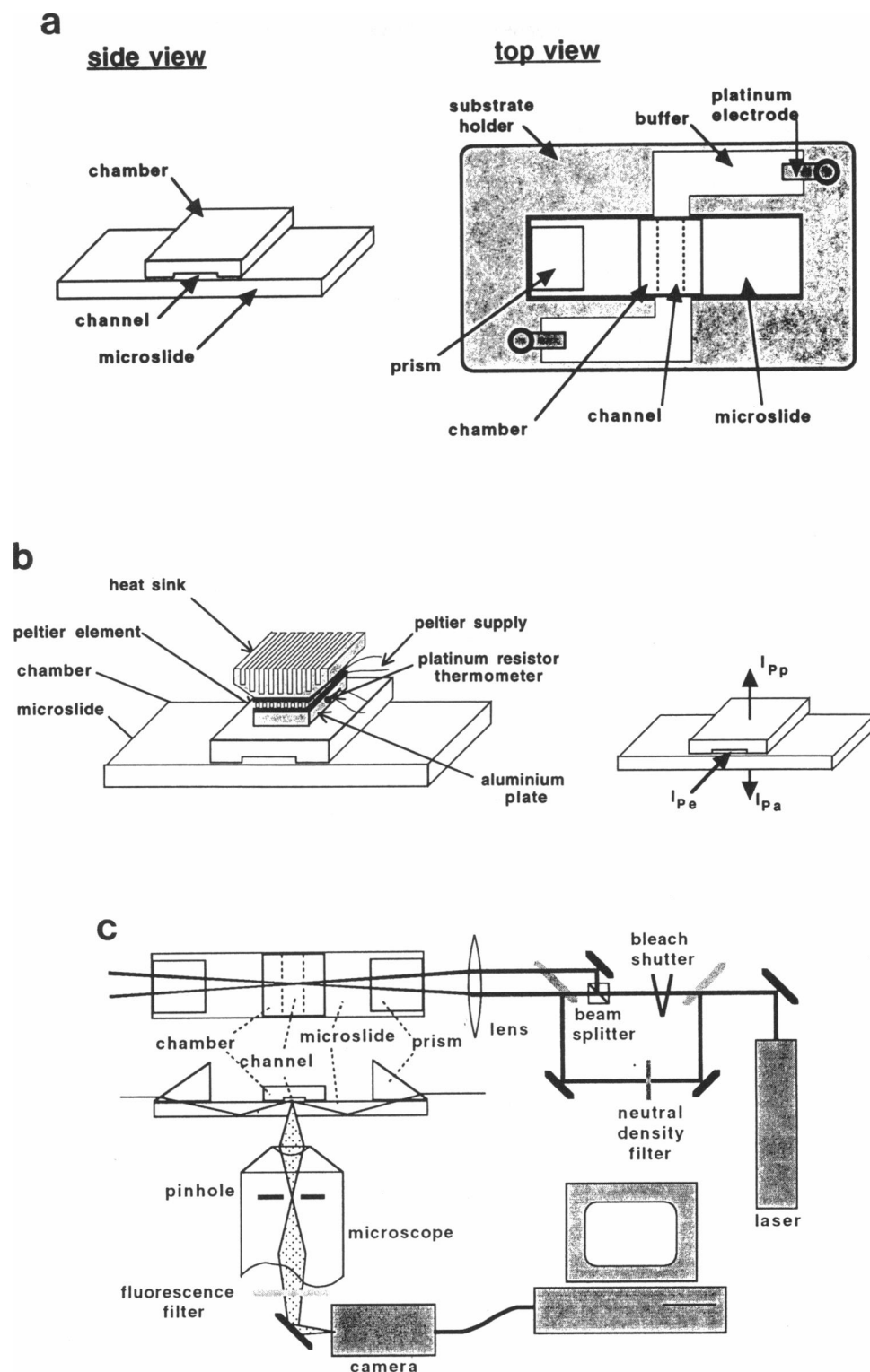


FIGURE 1 (a) Schematic view of the 2-D microelectrophoresis experiment. The supported bilayer is deposited onto the microslide. An electric field is applied on top of the bilayer and parallel to its plane along the narrow channel ($50\ \mu\text{m}$ high, $10\ \text{mm}$ wide, and $26\ \text{mm}$ long) by application of a voltage (0 – $1,000\ \text{V}$) between the two ends of the groove. (b) Schematic view of the Peltier element fixed on top of the chamber to control its temperature. The right side shows a diagram of the heat fluxes and the electrical power flow. See text for details. (c) TIR-FRAP set-up. An argon ion laser at $\lambda = 488\ \text{nm}$ is used as a light source (Innova 70; Coherent Inc., Palo Alto, CA). The light is coupled into the microslide, which acts as a waveguide, via a glass prism. The $\sin^2(x)$ pattern for bleaching is produced by interference of two laser beams of the same intensity. A part of the beam (10^{-4}) is deviated around the shutter and the beam splitter and is focused onto the observation area in order to observe the fluorescence after photobleaching. The microscope is an inverted type (Zeiss Axiomat; Carl Zeiss, Inc., Oberkochen, Germany). The setup, including the shutters and the CCD camera, is computer controlled.

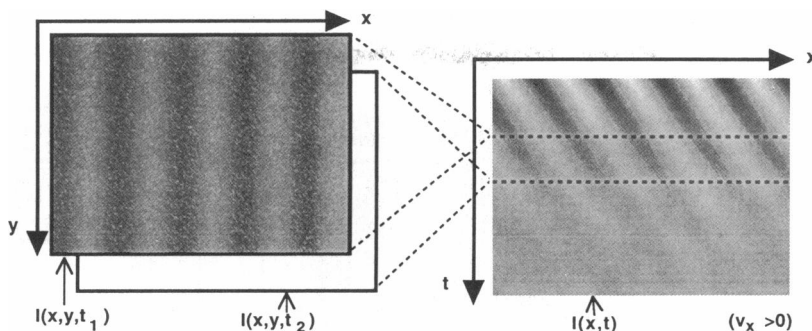


FIGURE 2 Method of evaluation. Snap shot fluorescence images are taken at time t_i after photobleaching. The wavelike intensity distribution $I(x, y, t_i)$ is averaged over the y direction. The distributions $I(x, t_i)$ are then plotted as a function of time as shown in the right image. The apparent fading away of the intensity profile in the $I(x, t)$ image caused by broadening of the wavelike patterns is determined by the lateral diffusion and yields the coefficient D . The deflection of the intensity maxima in the x direction corresponds to the electrophoretic motion of the charged fluorescent probes and yields the drift velocity $\langle v \rangle$.

wavelength of the bleached pattern is fitted to the function of Eq. 3. In the case of two differently charged lipids $c_k(t)$ is just the sum of $c_{1k}(t)$ and $c_{2k}(t)$. The fit is performed with the Levenberg-Marquardt algorithm described in detail in Numerical Recipes (Press et al., 1981). If not mentioned otherwise, the given errors are three times the standard deviations of the corresponding fit parameter.

Calculation of the temperature in the channel

With the model shown in Fig. 1 *b* (right), the heat fluxes and the resulting chamber temperature can be calculated from the dissipated electric power I_{pe} , the thermal conductivities k_g (chamber interior to the outer chamber surface) and k_a (chamber interior to the surrounding air), the temperature at the chamber surface T_s , and the temperature of the surrounding air T_a . The flux of electric power into the sample I_{pe} equals the sum of heat fluxes I_{pp} via the glass surface to the peltier element and I_{pa} via the glass surface of the microslide and the surrounding air

$$I_{pe} = -I_{pp} - I_{pa}. \quad (4)$$

Because of the small thickness of the 1-mm slides, the heat fluxes perpendicular to the surface dominate those parallel to the surface. The latter are therefore neglected in this calculation. The specific thermal conductivity of glass is 0.0138 W/cm °C. This yields a value of $k_g = 0.331$ W/°C using the values for the thickness $d = 1$ mm of the microslide and the area $a = 2.4$ cm² of the peltier element. The thermal conductivity $k_a = 0.0183$ W/°C was evaluated from a measurement of T_s vs. I_{pe} .

The heat fluxes are

$$I_{pe} = UI \quad (5a)$$

$$I_{pp} = k_g(T_s - T_{ch}) \quad (5b)$$

$$I_{pa} = \frac{k_a}{2}(T_a - T_{ch}). \quad (5c)$$

Only half of the surface of the chamber is in contact with the surrounding air so that the related thermal conductivity is $k_a/2$. The chamber temperature T_{ch} is

$$T_{ch} = \frac{I_{pe} + k_g T_s + \frac{k_a}{2} T_a}{k_g + \frac{k_a}{2}}. \quad (6)$$

For small fluxes of electric power up to 0.2 W, this difference is less than $\pm 0.5^\circ\text{C}$. For higher fluxes T_s can be varied to keep T_{ch} at a fixed value.

Electroosmosis and 2-D microelectrophoresis

During several experiments a significant transport of buffer through the microchamber was observed. This phenomenon is called electroosmosis (Hiemenz, 1986). If a charged surface, i.e., a lipid membrane containing molecules with charges and/or dipoles, is immersed in an electrolyte solution, an excess charge of oppositely charged ions will accumulate near the surface. The distribution of the ions is described by the Poisson-Boltzmann equation. Within a distance of several Debye lengths from the surface (perpendicular to the surface) the surface charge is screened by those oppositely charged and *mobile* electrolyte ions. Application of an electric field tangential to the charged surface causes a movement of the mobile ions and a flux of buffer [cm³/s] according to

$$V = \frac{EA\epsilon\epsilon_0\zeta}{\eta}, \quad (7)$$

where E is the electric field strength, A is the cross-section of the channel, ϵ is the dielectric permittivity of the buffer, η is its viscosity, and ζ is the zeta potential, i.e., the potential at a distance z_s at which the buffer velocity is zero, i.e., $|v| = 0$ for $z < z_s$ and $|v| > 0$ for $z > z_s$. This plane is called the "surface of shear." At z_s the buffer flow leads to a shear stress, which might result in a movement of the whole membrane.

The question arises whether electroosmotic flow of buffer has significant influence on the movement of lipid probes in bilayers. It also has to be discussed whether the observed migration of charged probes is substantially influenced by a possible movement of the whole membrane (bilayer or upper monolayer).

In this paper we describe experiments in which we studied (1) simultaneous drift of positively and negatively charged probes in one bilayer and (2) the movement of charged and uncharged probes in one bilayer. We show that the movement of the individual probe molecules can be separated from the movement of the total membrane. The mobility

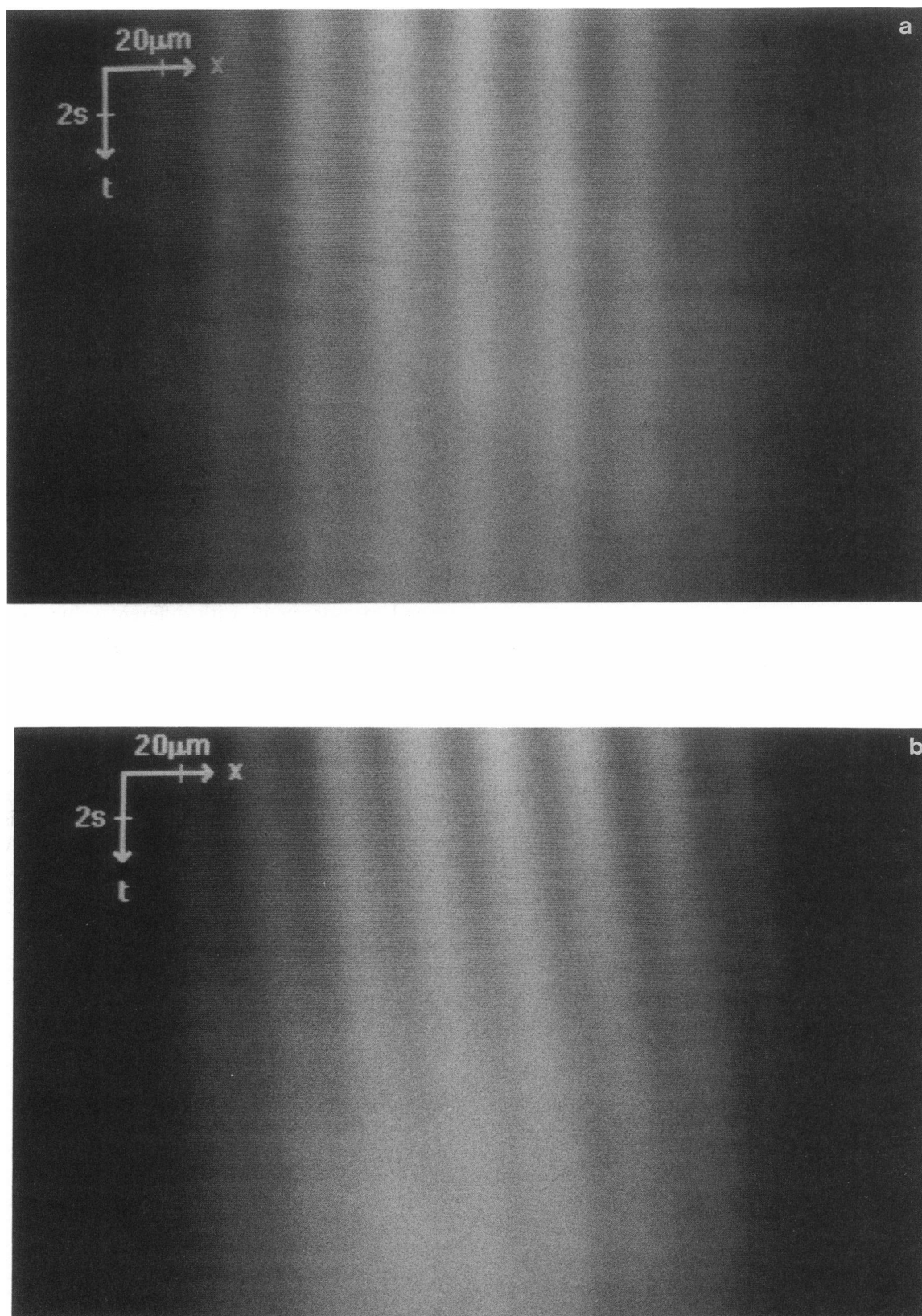


FIGURE 3 Examples of plots of fluorescence intensity distributions $I(x, t)$ in the absence (*a*) and presence (*b*) of an electric field. The membrane consisted of a DMPE monolayer containing 1.6 mol% of NBD-DPPE ($q = -e$), which was deposited onto silanized glass (hexadecyltrichlorosilane). Buffer conditions: 10 mM Tris, pH 8.5. The total measurement time is 29 s. The applied voltage is 0 V for *a* and 700 V ($E = 270$ V/cm) for *b*; $T_{\text{ch}} = 26.6^\circ\text{C}$. The shift of maxima in the x direction is determined by the drift velocity $\langle v_d \rangle$ parallel to the electric field direction, and the decay of the intensity maxima exhibits the diffusion coefficient. Data evaluation yields (*a*) $D = 1.14 \mu\text{m}^2/\text{s}$ and (*b*) $D = 1.68 \mu\text{m}^2/\text{s}$; $\langle v \rangle = 1.09 \mu\text{m}/\text{s}$.

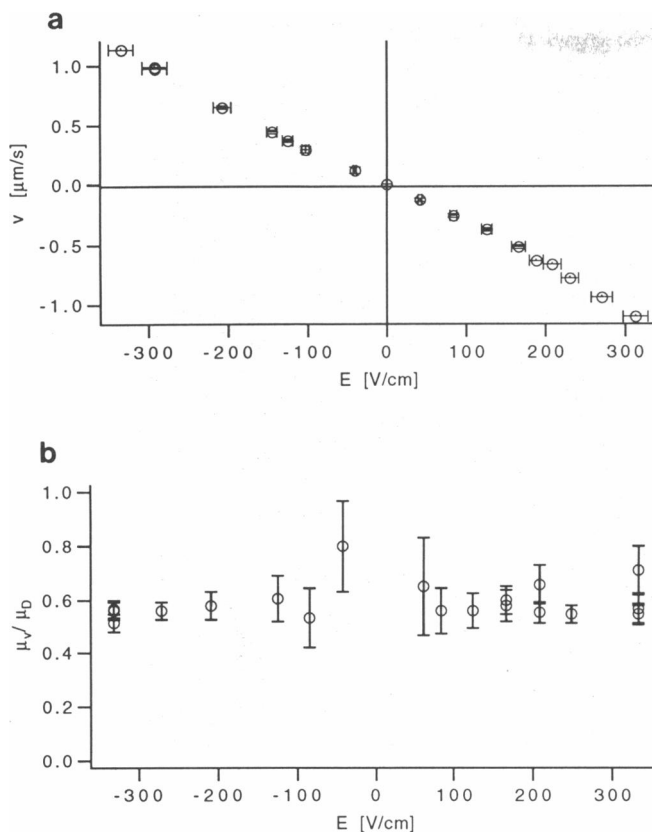


FIGURE 4 (a) Plot of average velocity $\langle v \rangle$ of charged lipid probe as a function of applied electric field. The system consists of: DMPE monolayer on silanized glass (hexadecyl-trichlorosilane) containing 1.6 mol% of NBD-DPPE; buffer: 10 mM tris, pH 8.5. (b) Plot of the quotient μ_v/μ_D as a function of E . μ_v is obtained from drift velocity in electric field ($\mu_v = \langle v \rangle / zeE$) and μ_D is obtained from the diffusion coefficients ($\mu_D = D/k_B T$). The quotient is constant, as expected from the Einstein relationship. However, the absolute value of μ_v is smaller than μ_D ($\mu_v \approx 0.6 \mu_D$).

coefficients μ_v and μ_D are calculated from the velocity v and the diffusion coefficient D , respectively. From these values an approximate value of the frictional force per molecule due to electroosmotic buffer flow can be calculated.

RESULTS AND DISCUSSION

Fig. 3 shows an example of 2-D microelectrophoresis measurements using NBD-DPPE (Fig. 9) as charged fluorescent probe. The system consists of a monolayer of DMPE¹ with 1.6 mol% of NBD-DPPE (lateral pressure 10 mN/m) deposited onto a silanized (hexadecyltrichlorosilane) glass microslide. Plots of the fluorescence intensity distributions $I(x, t)$ are displayed in Fig. 3 a for zero voltage and in Fig. 3 b for an applied voltage of 700 V (electric field strength $E = 270$ V/cm). Temperature at the outer chamber surface was 26.6°C in both cases.

¹L- α -Dimyristoyl-phosphatidyl-ethanolamine.

The fading away of the intensity “waves” due to diffusion and their additional lateral deflection in the presence of an applied field can be seen clearly.

For Fig. 3 a we obtained a diffusion coefficient of $D = 1.14 \mu\text{m}^2/\text{s}$ and for Fig. 3 b $D = 1.68 \mu\text{m}^2/\text{s}$. The average drift velocity in the second example was $\langle v \rangle = 1.09 \mu\text{m}/\text{s}$. In this experiment the temperature at the outer surface of the chamber was maintained constant. The calculated increase of the chamber temperature due to the dissipated electric power is $\Delta T \leq 0.5^\circ\text{C}$.

Fig. 4 a shows a plot of the average velocity $\langle v \rangle$ of the charged lipid probe as a function of applied field strength E . As expected for constant mobility $\mu_v = \langle v \rangle / zeE$, $\langle v \rangle$ varies linearly with E . The error in E indicated by horizontal bars results from variations of the thickness of the channel of $\sim 5\%$, which cause variations of the conductivity and therefore of E . The measurements were performed at different locations, so there is some uncertainty in E . The mobility was calculated from the measured average velocity according to $\mu_v = \langle v \rangle / zeE$ and from the diffusion coefficient D via the Einstein relationship $\mu_D = D/k_B T$. To check the validity of the Einstein relationship, the ratio μ_v/μ_D is plotted in Fig. 4 b for several measurements with different values of E . The error for values of E around zero is large, because μ_v is a quotient of two small numbers E and v . The ratio μ_v/μ_D does not depend on E as is expected, but the absolute value of μ_v is smaller than μ_D ($\mu_v \approx 0.6 \mu_D$). This latter value for the ratio was confirmed by experiments on 10 bilayers with between 10 and 50 measurements for each. This means that the effective force that acts on the probe molecules is smaller by a factor of ~ 0.6 than is calculated from field strength E and probe charge q (we used probes with $q = e$, $q = -e$, and $q = 0$) and/or there is an additional drift of the whole membrane versus the substrate.

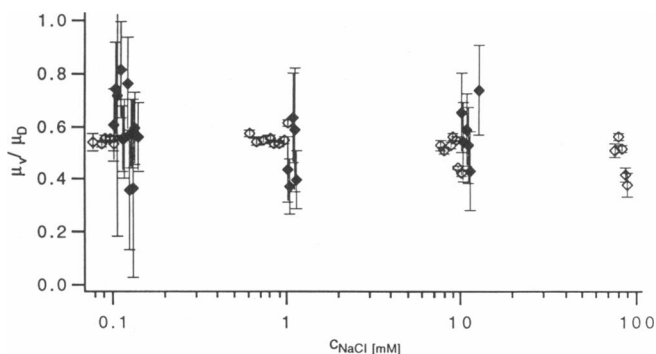


FIGURE 5 μ_v/μ_D measured for four different concentrations of sodium chloride in the buffer. Buffer: 1 mM Tris, pH 8.5, salt: NaCl. The concentrations are 0.1, 1, 10, and 100 mM NaCl. $T = 35^\circ\text{C}$ for the filled markers and 30°C for the others. The lowest concentration relates to unbuffered bi-distilled water with traces of ions. In this case, the concentration is deduced from the conductivity of the channel. For better visibility the data of each ion concentration are shifted.

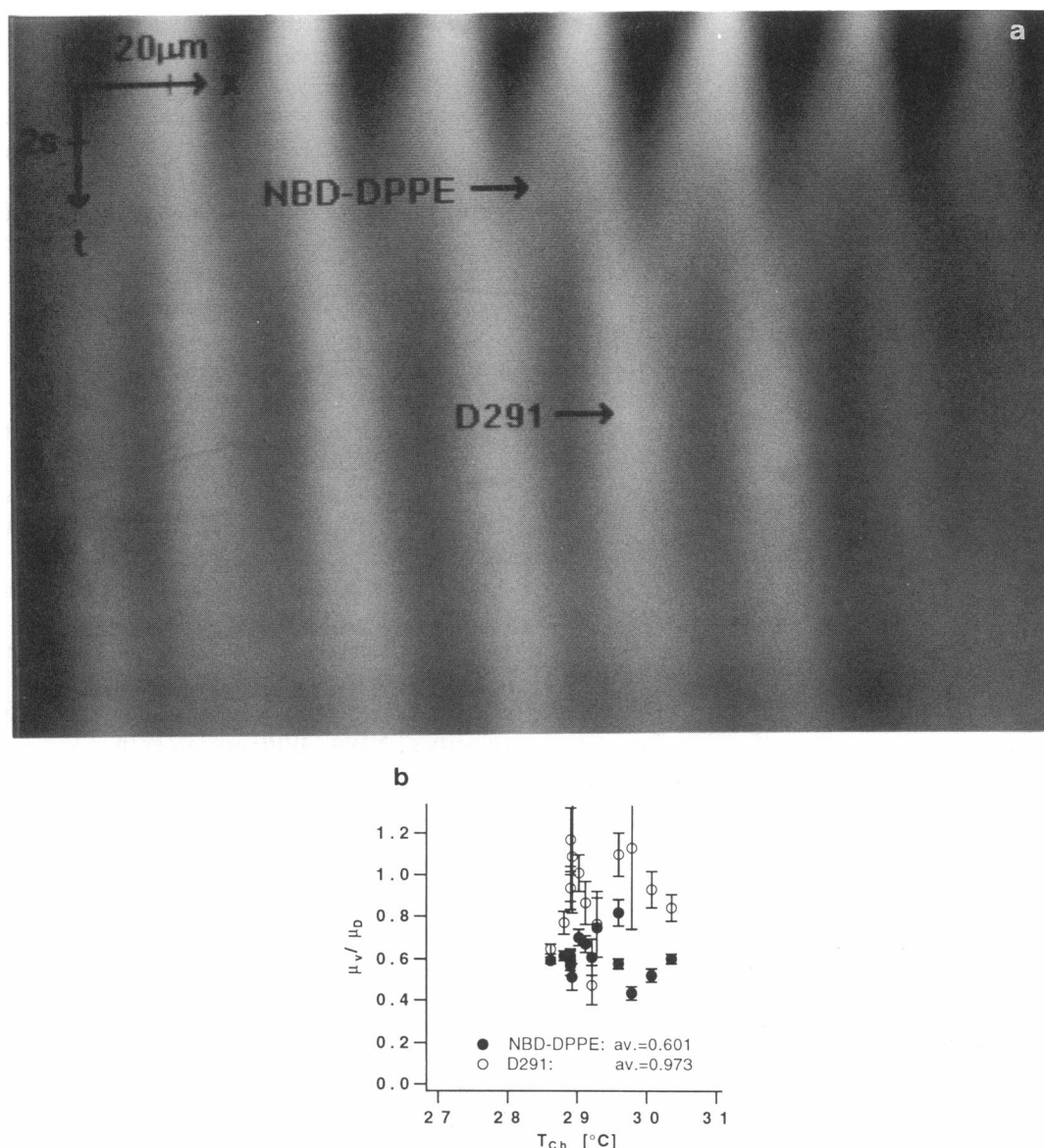


FIGURE 6 (a) 2-D microelectrophoresis experiment with a DMPC bilayer on a glass microslide containing two oppositely charged fluorescent amphiphiles: 2.5 mol% cationic D291 and 5 mol% anionic NBD-DPPE in the outer monolayer. The lateral pressure during monolayer transfer was 15 mN/m for each monolayer. Buffer composition: 2.5 mM Hepes, pH 7.0. The electric field is $E = 190$ V/cm. Note, first, that every intensity wave splits into one deflected to the right (D291) and one to the left (NBD-DPPE), and second, that the intensity profiles of the latter waves fade away much faster than those of the former. (b) The quotients of the mobilities μ_v/μ_D for each of the two fluorescent probes are plotted for different values of $|E|$ between 204 and 445 V/cm. The temperature was calculated from the measured T values at the surface and the dissipated electrical power. See text for details.

There are several possible explanations for this finding that have to be discussed: (a) Bleaching during the measurement by the observation beam leads to an overestimation of the diffusion coefficient and consequently the value of μ_D would be too large. This effect certainly depends on the sensitivity of the fluorescent dye. It can be evaluated from the zero order component $c_{k=0}(t)$ of the Fourier transform of the measurement. In our experiments we used two rather sensitive (NBD-DPPE and D70) and a quite stable dye (D291). The bleaching constant in our measurements results in a maximum rela-

tive error $(\Delta D/D)_{\text{bleach}}$ of 5% in the case of NBD-DPPE and even smaller for D291. Thus, we rule out this error source.

(b) The ion concentration in the buffer influences the ratio μ_v/μ_D . The cloud of counterions around the probe charge has to continuously rearrange during the movement of the charged probe. It is therefore not in equilibrium and a so-called *relaxation field* E_R is produced that opposes E . This relaxation effect is discussed in standard texts, for example, Falkenhagen (1971), Hunter (1981), and Hiemenz (1986). It should become negligible as the

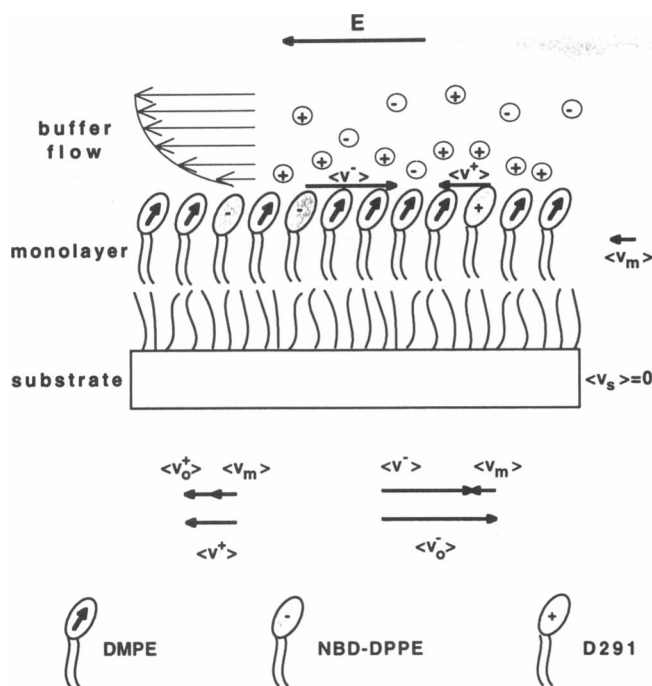


FIGURE 7 Sketch of a monolayer on silanized glass. The relation between the apparent drift velocities $\langle v^+ \rangle$ of the probes and their velocities relative to the membrane $\langle v_o^+ \rangle$ are indicated in the case of negative ζ potential. $\langle v_m \rangle$ is the velocity of the whole membrane.

Debye length becomes large (ionic strength becomes low) and in the case of small probe velocity, i.e., small mobility of the probe compared with the mobility of the counterions.

Fig. 5 shows that the ratio μ_v/μ_D does not depend appreciably on the concentration of ions in the buffer. The lowest concentration given in this graph relates to unbuffered bi-distilled water with traces of ions. In this case, the concentration is deduced from the conductivity of the channel. The large errors for the data displayed as filled markers result from a weak fluorescence intensity and therefore a poor signal/noise ratio.

(c) Electroosmotic flux of buffer through the chamber will lead to a frictional force. The flux of buffer is also proportional to the applied field strength (Eq. 7). The influence of this type of force has been deduced from experiments using oppositely charged probes. For such a system, the frictional force would increase the effective force acting on one probe and decrease the effective force acting on the oppositely charged probe. The direction of electroosmotic flow depends on the sign of the ζ potential at the lipid/water interface. It can be controlled by the composition of the lipid membrane.

To check the influence of frictional forces from electroosmotic flux on the ratio μ_v/μ_D , and to ensure that the observed motion is due to the movement of single probes, we performed the following experiments with two different probes in one membrane.

Fig. 6 *a* shows the 2-D microelectrophoresis experiment for a system containing two oppositely charged lipids (NBD-DPPE, 5 mol%; D291, 2.5 mol%; see Fig. 9) of different molecular weight and chain length in the outer monolayer of a DMPC² bilayer (lateral pressure for each monolayer during transfer: 15 mN/m). It can be clearly seen that the two oppositely charged fluorescent probes migrate in opposite directions. This shows that the motion is driven mainly by the electric field. Frictional forces due to buffer flow induced by electroosmosis would cause a uniform movement of the whole membrane and the probes within regardless of the sign of charge they bear.

The situation may be completely different with large membrane probes with large hydrophilic head groups extending into the aqueous phase. In this case frictional force may easily dominate charge effects, as has been demonstrated by McLaughlin and Poo (1981).

As demonstrated in Fig. 6 *a*, the intensity profile of the NBD-DPPE probe fades away faster than that of the D291 fluorescent dye. Furthermore, the deflection angle of the former probe is larger than that of the latter. This shows that the diffusion coefficient and the average drift velocity of NBD-DPPE are larger than those of D291. As shown in Fig. 6 *b* the ratio μ_v/μ_D is ~ 1 for D291 and again ~ 0.6 for NBD-DPPE as in case of Fig. 4 *b*.

Negative ζ potential causes an accumulation of positive buffer ions near the interface (Fig. 7). Electroosmotic buffer flow thus leads to a frictional force that may induce a motion of the whole membrane versus the substrate (velocity $\langle v_m \rangle$) and tends to slow down negatively charged probes like NBD-DPPE and accelerate positively charged probes like D291. The velocity $\langle v_m \rangle$ then has to be subtracted from the measured velocity of positively charged probes $\langle v^+ \rangle$ and added to the measured velocity of negatively charged probes $\langle v^- \rangle$ according to

$$\langle v_o^+ \rangle = \langle v^+ \rangle - \langle v_m \rangle \quad (8a)$$

$$\langle v_o^- \rangle = \langle v^- \rangle + \langle v_m \rangle \quad (8b)$$

to yield the velocities of the probe molecules relative to the membrane $\langle v_o^+ \rangle$ and $\langle v_o^- \rangle$, respectively. μ_v/μ_D calculated from $\langle v_o^+ \rangle$ or $\langle v_o^- \rangle$ should then hold the Einstein relationship.

The velocity $\langle v_m \rangle$ of the membrane was evaluated in an experiment with NBD-DPPE (2.5 mol%) and the uncharged lipid probe D70 (2.5 mol%) in the outer monolayer of a DMPC bilayer. No electric force will act on D70. Its drift velocity $\langle v \rangle$ is equal to the velocity $\langle v_m \rangle$ of the total membrane. Fig. 8 shows a typical fluorescence pattern $I(x, t)$ of such an experiment. The profile $I(x, t)$ at $t = 0$ (immediately after bleaching) splits into two bands: one is deflected from the vertical, whereas the

²L- α -Dimyristoyl-phosphatidyl-choline.

TABLE 1 Summary of mobilities μ and diffusion coefficients D of lipid probes

Bilayer (first/second monolayer)	HTS*/DMPE	DMPC/DMPC	DMPC/DMPC
Probe(s) (in second monolayer)	NBD-DPPE	NBD-DPPE/D291	NBD-DPPE/D70 ⁵
Charge(s)	-e	-e/+e	-e/0
Molecular weight(s)	768	768/489	768/404
Temperature (°C)	27 ± 0.5/30 ± 0.5	30 ± 0.5	37.3 ± 1
D ($\mu\text{m}^2/\text{s}$)	1.2 ± 0.3/3.5 ± 0.5	4.4 ± 0.5/0.9 ± 0.2	5.6 ± 1/7.0 ± 1
μ_v ($\mu\text{m}^2/eVs$)	31 ± 3/75 ± 10	95 ± 10/35 ± 5	140 ± 10/—

* Hexadecyltrichlorosilane.

other is nearly immobile. This shows that $\langle v_m \rangle$ is small compared with the velocity of a small lipid probe with $|q| = e$ like NBD-DPPE. However, more elaborate numeric evaluation actually shows a slow movement even of the uncharged D70 (see Fig. 9). We assume that the coupling of the small probe D70 to the membrane is much stronger than to the aqueous phase, and that its velocity v_{D70} therefore yields $\langle v_m \rangle$. The velocity is $v_{D70} = 0.42 \mu\text{m/s}$ in the direction of the electrical field, whereas for NBD-DPPE it is $v_{\text{NBD-DPPE}} = 2.7 \mu\text{m/s}$ in the *opposite* direction. From this result we conclude that the ζ potential is negative for this particular membrane composition. The velocities are average values of several measurements with field strength $E = 208 \text{ V/cm}$ and temperature $T_{\text{ch}} = 37.3^\circ\text{C}$.

A correction of μ_v/μ_D based on the observed value of $v_{D70} = \langle v_m \rangle$ could explain the differences of μ_v/μ_D from the measurements obtained for the two oppositely charged probes (Fig. 6 *b*), assuming the conditions are comparable. Ratios of μ_v/μ_D of ~ 0.7 for NBD-DPPE and ~ 0.8 for D291 are expected. The values of the diffusion coefficients and the mobilities are summarized in Table 1.

Concluding remarks

The 2-D microelectrophoresis opens new possibilities for the application of supported bilayers (e.g., in biosensors). Thus, as suggested previously (Stelzle and Sackmann, 1989), it enables the accumulation of charged amphiphiles (receptors) near electrodes. To improve the

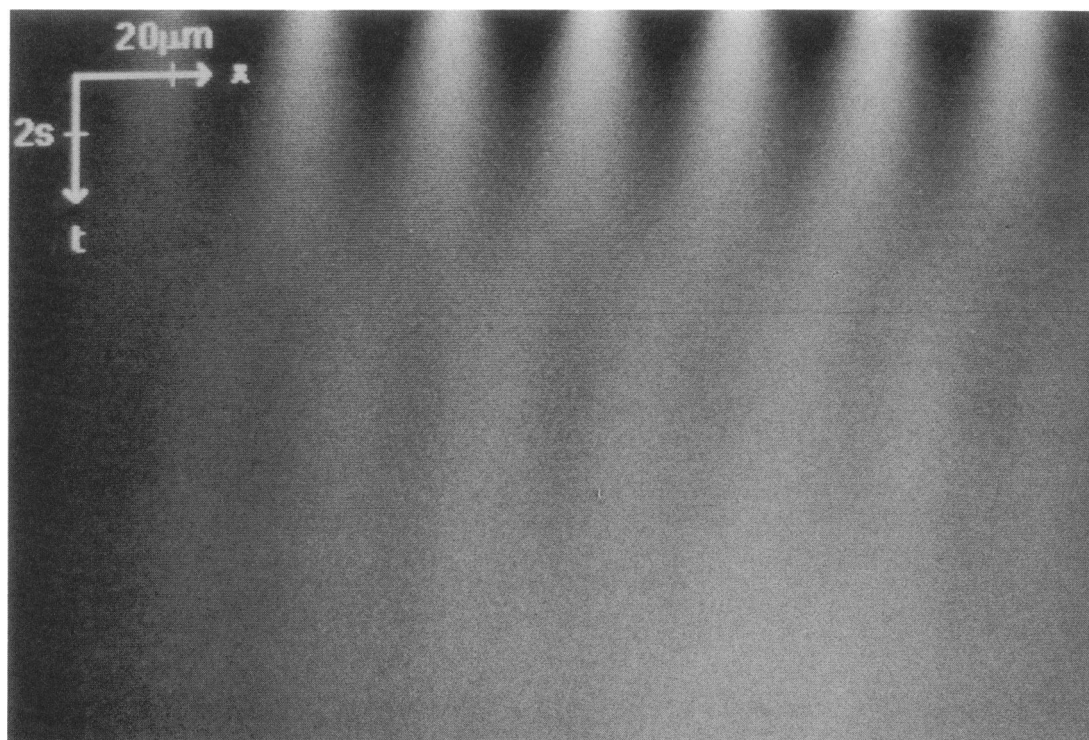
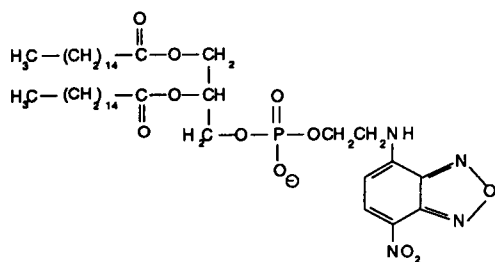
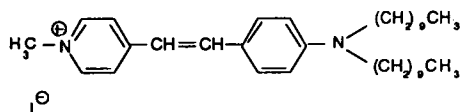


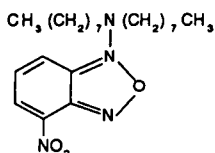
FIGURE 8 Experiment with negatively charged NBD-DPPE (2.5 mol%) and uncharged D70 (2.5 mol%) in the outer monolayer of a DMPC bilayer. Lateral pressure during monolayer transfer was 15 mN/m for each monolayer. Buffer: 5 mM Hepes, 5 mM NaCl, pH 7.0. Note the presence of two fractions, one of which is deflected to the left and simultaneously broadened, whereas the other remains at the same x position and is only broadened.



NBD-DPPE, $q=-1e$
(N-(7-nitrobenz-2-oxa-1,3-diazol-4-yl)
dipalmitoyl-L- α -phosphatidylethanolamine)



D291, $q=+1e$
(4-(4-didecylaminostyryl)-N-methylpyridinium iodide)



D70, $q=0$
(4-(N,N-diethyl)amino-7-nitrobenz-2-oxa-1,3-diazole)

FIGURE 9 Charged and uncharged fluorescent amphiphilic dyes used in 2-D microelectrophoresis experiments.

selectivity of sensors, different types of receptors as well as charged and uncharged receptors of one type after addition of the ligands could be separated by this technique.

In addition, the presented techniques enable studies of friction between monolayers and of more fundamental problems of electrophoresis in membranes.

It is a pleasure to thank Dr. Hermann Gaub for helpful discussions.

The work was supported by the Deutsche Forschungsgemeinschaft (SFB 266, projects C1 and D3), the Bundesministerium für Forschung und Technologie (BMFT), and the Fonds der Chemischen Industrie.

Received for publication 2 December 1991 and in final form 11 June 1992.

REFERENCES

- Eggl, P., D. Pink, B. Quinn, H. Ringsdorf, and E. Sackmann. 1990. Diffusion in quasi two-dimensional macromolecular solutions. *Macromolecules* 23:3472-3480.
- Falkenhagen, H. 1971. *Theorie der Elektrolyte*. Hirzel Verlag, Stuttgart, 148-168.
- Hiemenz, P. C. 1986. Electrophoresis and other electrokinetic phenomena. In *Principles of Colloid and Surface Chemistry*. P. C. Hiemenz, editor. Dekker, Marcel Inc., New York. 737 pp.
- Hunter, R. J. 1981. *Zeta Potential in Colloid Science*. Academic Press, New York. 98 pp.
- Langmuir, I. L., and V. J. Schaefer. 1938. *J. Am. Chem. Soc.* 60:1351-1360.
- McLaughlin, S., and M. Poo. 1981. The role of electro-osmosis in the electric-field-induced movement of charged macromolecules on the surface of cells. *Biophys. J.* 34:85-93.
- Merkel, R., E. Sackmann, and E. Evans. 1989. Molecular friction and epitactic coupling between monolayers in supported bilayers. *J. Physiol. (Paris)*. 50:1535-1555.
- Press, W. H., B. P. Flannery, S. A. Teukolsky, and W. T. Vetterling. 1981. *Numerical Recipes in C*. Cambridge University Press, Cambridge. 542-557.
- Smith, B. A., and H. M. McConnell. 1978. Determination of molecular motion in membranes using periodic pattern photobleaching. *Proc. Natl. Acad. Sci. USA*. 75:2759-2763.
- Stelzle, M., and E. Sackmann. 1989. Sensitive detection of protein adsorption to supported lipid bilayers by frequency-dependent capacitance measurements and microelectrophoresis. *Biochim. Biophys. Acta*. 981:135-142.
- Thompson, N. L., T. P. Burghardt, and D. Axelrod. 1981. Measuring surface dynamics of biomolecules by total internal reflection fluorescence with photobleaching recovery or correlation spectroscopy. *Biophys. J.* 33:435-454.
- Von Tscherner, V., and H. M. McConnell. 1981. Physical properties of lipid monolayers on alcyated planar glass surfaces. *Biophys. J.* 36:421-427.
- Zimmermann, R. M., C. F. Schmidt, and H. E. Gaub. 1990. Absolute quantities and equilibrium kinetics of macromolecular adsorption measured by fluorescence photobleaching in total internal reflection. *J. Colloid Interface Sci.* 139:268-280.